ICES Journal of Marine Science, 58: 985–993. 2001
doi:10.1006/jmsc.2001.1095, available online at http://www.idealibrary.com on IDEAL®

Modelling the effect of a slope-water intrusion on advection of fish larvae in May 1995 on Georges Bank

J. P. Manning, R. G. Lough, C. E. Naimie, and J. H. Churchill

Manning, J. P., Lough, R. G., Naimie, C. E., and Churchill, J. H. 2001. Modelling the effect of a slope-water intrusion on advection of fish larvae in May 1995 on Georges Bank. – ICES Journal of Marine Science, 58: 985–993.

In the spring of 1995, an intrusion of warm/salty slope water occurred on the southern flank of Georges Bank. As observed on several cross-bank hydrographic and acoustic Doppler current profiler sections, this intrusion resulted in a narrow (10 km) but intense shelfbreak jet (30 cm s^{-1} westward residual) in the near-surface waters. A satellite tracked drifter with a drogue located in the core of this jet (15 m) travelled 120 km to the west in 5.5 d. To examine this process and demonstrate the potential redistribution of fish larvae (collected with bongo net hauls) in the presence of a slope-water intrusion, a finite-element 3D circulation model has been initialized with the observed CTD density field. Moored velocity records are assimilated into the model to estimate the oceanic boundary elevations of a limited-area grid. The simulated particle tracks indicate enhanced along-bank flow relative to the long-term seasonal mean and a downwelling convergence zone in the vicinity of the shelf/slope front. The model resolves most of the subtidal flow and provides insight into the vertical advection of the animals and potential mechanisms of retention and loss.

Keywords: advection, fish larvae, modelling, Georges Bank, shelfbreak jet, drifters.

J. P. Manning and R. G. Lough: NOAA/NMFS, Woods Hole, MA 02543, USA. C. E. Naimie: Dartmouth College, Hanover, NH 03755, USA. J. H. Churchill: Woods Hole Oceanographic Institution, Woods Hole, MA 02543, USA. Correspondence to J. P. Manning: e-mail: jmanning@whsun1.wh.whoi.edu

Introduction

The endeavour to follow a concentration of fish larvae on Georges Bank and to sample the same population over the period of several days continues to challenge those interested in trophodynamics of the species. The tendency for fish larvae and their prey to converge along frontal structures and the fact that these frontal structures are translated and distorted over the M2 tidal cycle results in a very dynamic system that is difficult to sample (Franks and Chen, 1996; Franks and Walstad, 1997). The first major multi-ship effort of this nature on Georges Bank occurred with the "patch study" in the fall of 1978 (Lough and Trites, 1989). OPEN 1, another major effort, was conducted more recently on the nearby Scotian Shelf (Griffin and Thompson, 1996), where circulation modeling and data assimilation were used to follow a concentration of cod larvae. The 1988–1989 frontal study (Perry *et al.*, 1993) on the northern flank of Georges Bank also addressed the problem of sampling in the presence of strong cross-bank gradients. Many of the process studies of the Global Ecosystem Dynamics (GLOBEC) programme on Georges Bank (1994–1999) had similar objectives: to sample the water column in a Lagrangian reference frame over the cruise period.

One of the overall objectives of GLOBEC is to examine the role of various mesoscale features in determining cross-shelf and along-shore transport of meroplankton, holoplankton, and ichthyoplankton. The physical processes that may generate these mesoscale features include a seemingly chaotic combination of surface heating (Mountain *et al.*, 1996), wind (Greenberg *et al.*, 1997), instabilities along the tidal (Loder and Wright, 1985) and shelf-slope (Garvine *et al.*, 1988; Houghton *et al.*, 1988) fronts, highly variable shelf-break jets (Linder, 1996; Pickart *et al.*, 1998), effects from Gulf Stream rings (Garfield and Evans, 1987), and advection of upstream source waters (Bisagni *et al.*, 1996; Houghton *et al.*, 1979). All these processes result in episodic perturbations of the M2 tidal flow on Georges Bank and occur at a wide range of spatial scales such that modeling efforts to date have failed to simulate most of the subtidal variability. However, recent efforts in coastal circulation modeling have incorporated more realistic, highly resolved bathymetry, initial conditions, turbulence formulations, and forcing which have

1054–3139/01/050985+09 $35.00/0

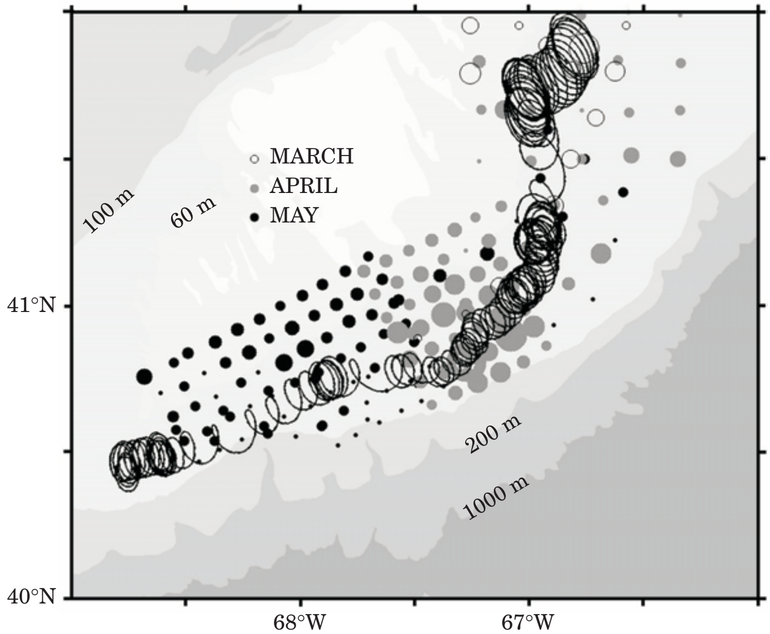

Figure 1. Number of cod larvae 100 m^{-3} as observed by bongo net hauls on three cruises (SJ9503, SJ9505, and SJ9507) overlaid on a numerical particle track as modeled by a barotropic, wind-driven, M2 tidal flow.

resulted in significant improvements. The application of these models as practical tools in fisheries oceanography is now a more realistic approach to the investigation of larval transport in 3D flow fields.

Our purpose is to demonstrate the use of one of these models (Lynch *et al*., 1996; Lynch and Hannah, 2001) in describing a particular mesoscale feature that was observed during mid-May 1995 on the southern flank of Georges Bank. While the observations alone provide an interesting view of an anomalous event, the model initialized with the atypical density field is used to describe the potential consequences as they relate to the larval advection. The event is an intrusion of slope water up into shallow (65 m) portions of the shelf, which, according to satellite imagery, was apparently due to a Gulf Stream ring approaching from the east. We distinguish between observations and modeling aspects throughout.

Methods

Observations

GLOBEC process studies in the spring of 1995 included a series of fish larvae surveys in March, April, and May (Figure 1). We focus on mid-May, when the RV "Seward Johnson" (SJ9507) conducted a fine-scale grid of cross-bank sections on the southern flank with 7-nm station spacing. The purpose of the SJ9507 grid was to map the distribution of cod and haddock larvae in relation to the oceanographic conditions [Figure 2(a)]. The animals were collected on an oblique bongo-net tow with a SEABIRD model 19 CTD attached to the wire. The nets were 333 and 505 µm mesh. In addition, a set of MOCNESS (Multiple Opening and Closing Net Environmental Sampling System) tows was conducted immediately following the bongo tows to estimate the vertical distribution of larvae. At the same time, the RV "Katadin" and RV "Albatross IV" conducted similar operations over progressively broader scale regions of the bank. A combined total of 160 CTD casts (Figure 3) were conducted on Georges Bank from 8 to 18 May 1995. ADCPs were operating on three vessels. A total of 11 ARGOS/GPS/VHF drifters deployments with drogues (1.6 × 6 m) tethered at 10-m depth were made on SJ9507. Four of these deployments were made during the fine-scale grid and are discussed here.

Two GLOBEC moorings (STI and ST2) were in place and located within the easternmost transect [Figure 2(a)] of the grid survey. These had current meters attached at multiple depths as well as temperature and salinity sensors. The current records from ST2 are used later under model assimilation and validation discussion. The hourly wind record from an anemometer mounted on ST1 is used to drive the model. Windstress was calculated by the method of Large and Pond (1981) and linearly interpolated to each time step.

Modelling

The Dartmouth Circulation Model (Lynch *et al.*, 1996) is a 3D finite element time-stepping model with atmospheric and boundary forcing. In its prognostic mode, it includes a free surface with terrain following vertical coordinates, resolves surface and bottom boundary layers using advanced turbulence closure, and transports temperature and salinity. The model was run on a grid which includes all of Georges Bank, but is limited to water depths less than 150 m. There are 1200 grid points in the horizontal and 21 levels in the vertical. The basic model was forced by observed winds and tidal elevations (five constituents) at the boundaries.

Model runs were conducted with increasing sophistication. The first runs were conducted to simply estimate M2 tides for the 3D flow field. These were used in deriving a residual flow as observed by ADCP records. Secondly, runs were made on a homogenous density field (barotropic) for a two-month period to examine the combined effect of the M2 tide and the observed wind. Beginning at the site of highest egg densities in mid-March, water parcels were tracked to the Great South Channel in mid-May (Figure 1). Third, the model was run to include the observed density field and the diagnostic velocity [as estimated by FUNDY5, another of the Dartmouth model suites as described in Lynch *et al.* (1992)]. This QUODDY (Lynch *et al.*, 1996) baroclinic model is run with a 180 s time-step for a week (11–18 May). Fourth, the CASCO model (Lynch and Hannah, 2001) was implemented to make estimates of the time-varying (subtidal) elevations along the boundary of the grid. These elevations were obtained by assimilating moored velocity records from three different depths at ST2. The purpose of this operation is to simulate the potential effect of the offshore (oceanic) forcing on the interior of the grid. More details associated with the assimilation method used are provided in the appendix.

Each of the bongo net and satellite-tracked drifter observations are tracked (Blanton, 1993) through the 3D baroclinic flow field subsequent to the time of sampling and deployment, respectively. The numerical drifters were initialized at multiple depths ranging from 5 to 45 m below the surface in intervals of 5 m and were allowed to advect passively throughout the water column. For the purpose of comparing with observed drifter tracks some numerical drifters were held constant at particular drogue depths.

We have implemented an optimal interpolation technique that projects the hydrographic observations on to the model grid. The gridding procedure incorporates the

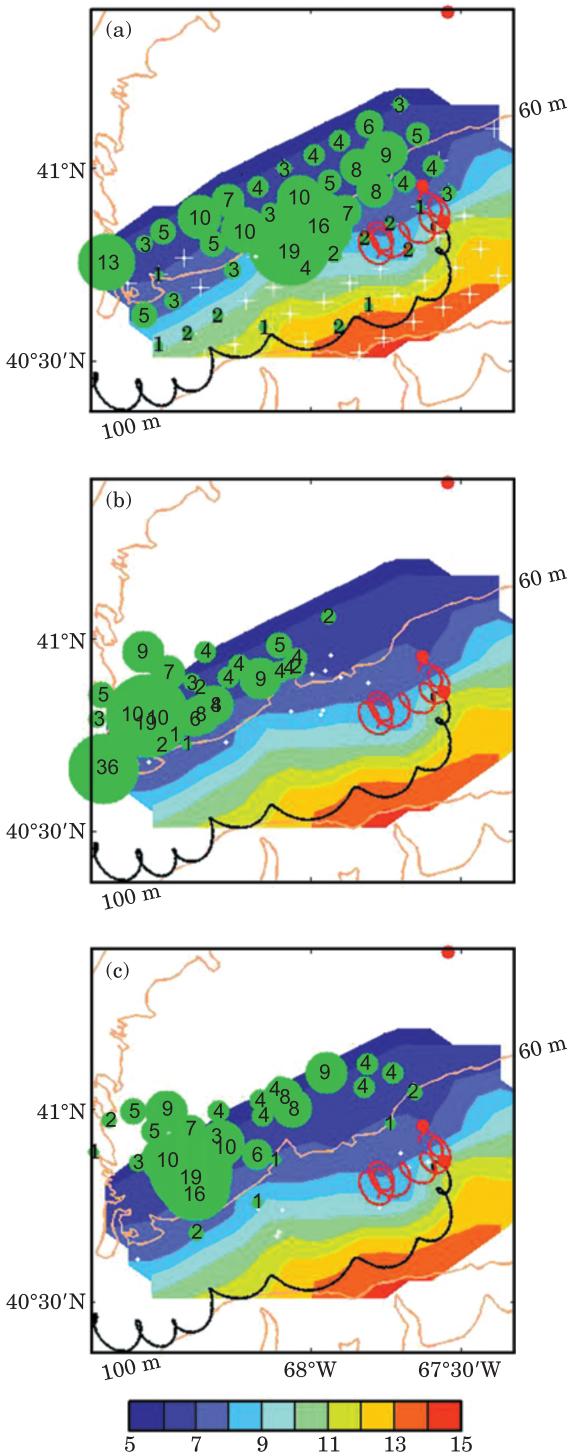

Figure 2. The displacement of cod larval concentrations caused by slope-like water intruding onto Georges Bank: (a) number of larvae 100 m^{-3} as observed (11–14 May, 1995; green circles) and after advection (17 May) by the model of particles that began at (b) 15 m or (c) 45 m. CTD bottom temperatures are contoured, two satellite tracked drifter paths are depicted as thin lines (red and black) and mooring locations are shown as red dots. Note the general convergence near the 8 isotherm after 6 d compared with the observed distribution.

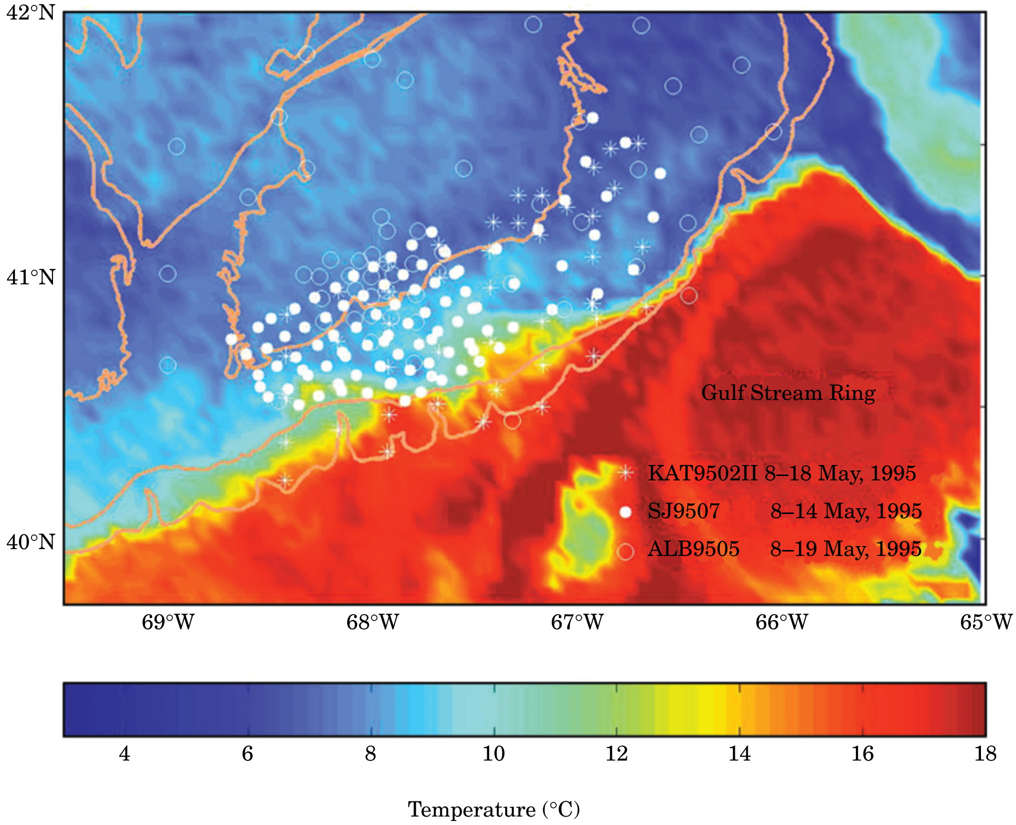

Figure 3. CTD cast conducted between 8 and 19 May 1995 on Georges Bank from three different vessels on satellite-imaged surface temperatures (21 May, 1995 @0134Z) depicting the effect of a Gulf Stream ring on the southern flank (brown lines: 60-m 100-m, and 200-m isobaths).

anisotropic nature of the field variables with an elliptic search pattern dependent on the local bathymetric gradients (Hannah *et al.*, 1996). Cross-bank (S_x) and along-bank (S_y) correlation scales were derived from:

$$S_x = S_0\ (1 - C_x\ s)$$

$$S_y = S_0\ (1 - C_y\ s)$$

where $S_0 = 30$ km, $C_x = 3$ km, $C_y = 10$ km, and s is the local non-dimensional bathymetric gradient (based on nearby model grid nodes). Hence, we are imposing an assumption about the topographically aligned frontal structures. The vertical search radius (S_z) was set to 15 m. The temporal search radius (S_t) was set to 30 d, more than the time span of the data. The resulting OAX observed fields from mid-May 1995 were compared to the OAX climatological fields from May/June historical archives. These climatological fields (Naimie *et al.*, 1994) were produced from the Canadian AFAP database (Petrie *et al.*, 1996).

Results

Observations

Given a sequence of clear satellite images (approximately one per week during the period of April–June 1995), we were able to detect the passage of a Gulf Stream warm core ring. The image of 26 April showed the sharp meander in the Gulf Stream, which eventually breaks off (5 May) in the form of a ring. The ring appears to generate instabilities with its forward edge intruding water up on the southern flank of the bank (cf. May 21; Figure 3).

Similarly, a sequence of cross-bank vertical sections could be generated from the various shipboard surveys in the southern flank. Figure 4 shows the evolution of the intrusion event as it was observed along the 68°W with the foot of the front (34 PSU) extending all the way to the 65 m isobath in mid-May. This is compared to the historical average conditions presented in the top panel.

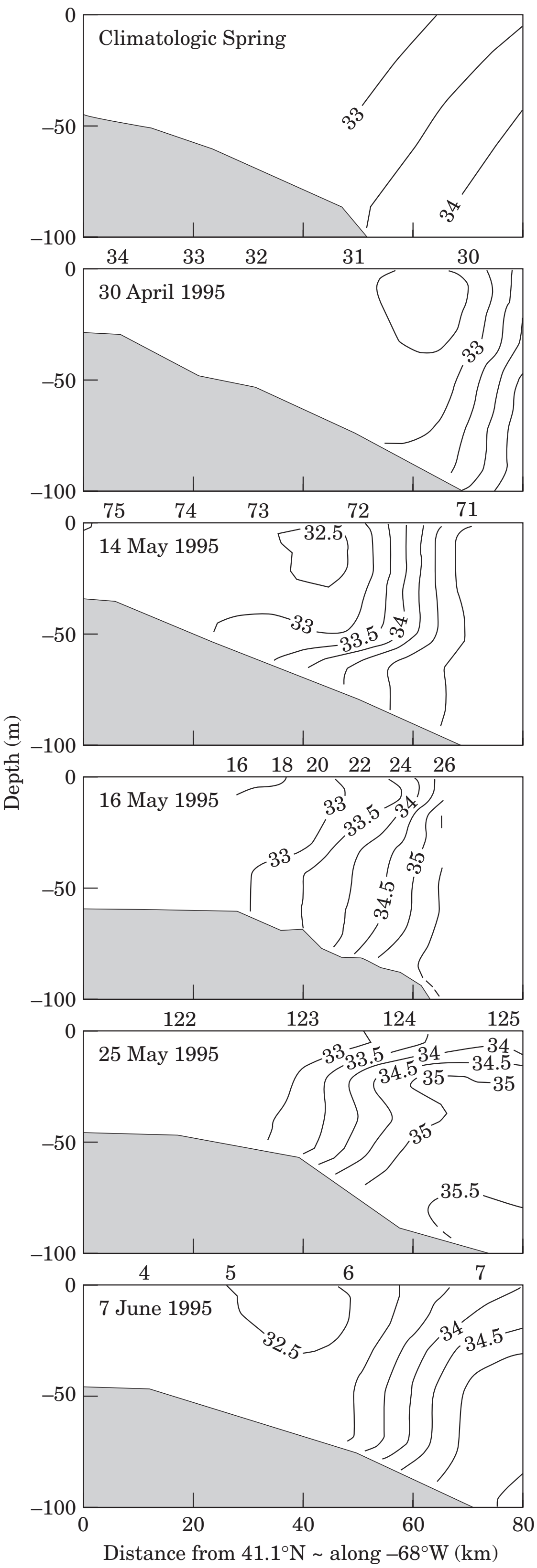

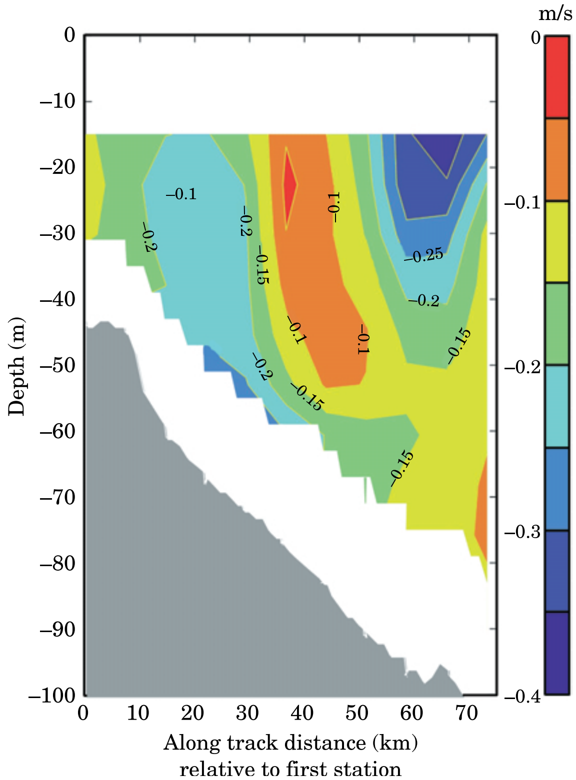

Figure 5. Detided 150 kHz ADCP E/W velocity at a cross-bank section (in the vicinity of moorings; see Figure 2) taken on 4 May 1995 (EN266), showing the band of westward flow on the off-bank edge of the transect and an additional band in the region of the tidal front near the 60-m isobath (white: insufficient data return; grey: southern flank of Georges Bank). The along-bank velocity has been detided by subtracting the Dartmouth Model 3D M2 tides.

The most complete observation of the shelf-break jet was made earlier in May 1995 (Figure 5), while the RV "Endeavor" was steaming along the second transect from the east in Figure 2(a) (near the moorings). In this case, the near-surface (15 m) detided flow was more than 35 cm s^{-1} towards the west. One of the four drifters deployed during the first two legs of the SJ9507 fine-scale grid was advected along at 29 cm s^{-1} (thin black line in Figure 2) while others moved sluggishly at 2–3 cm s^{-1} on the bankward side of the jet.

The distribution of larvae in mid-May was concentrated just bankward of the intruding shelf-slope front

Figure 4. Observed evolution of the intrusion event along the 68°W (as measured in terms of salinity; psu) with the foot of the front extending all the way to the 65-m isobath in mid-May (numbers at the top refer to CTD cast numbers). The uppermost panel represents a comparison with the average May–June situation according to the Atlantic Fisheries Assessment Program (Petrie *et al.*, 1996) database (top panel).

[Figure 2(a)]. The outer shelf was exposed to slope water intrusion and enhanced along-bank flow and consequently void of animals. This is in contrast to the distribution approximately one month earlier, when the highest concentrations were on the edge of the shelf near the 90 m isobath (Figure 1).

Modelling

While the model can obviously be run with a variety of inputs to test a multitude of hypotheses, the results described here address a few specific questions. First, as noted above, the simple tidal model was implemented to resolve a shelf-break jet after subtracting the output from the ADCP-recorded velocity. While this detiding procedure is far from rigorous, the magnitude of the residual flow is supported by drifter observations.

Second, the barotropic model (driven by both tides and wind) estimates a two-month advection of particles from the Northeast Peak (Figure 1) of Georges Bank. This run provides support to the notion that the cohorts observed in April were the same as those observed earlier in March. Those observed in May, however, are less likely to belong to the same population. Only those particles bankward of the shelf-break jet system could possibly be retained on the bank.

The model was then run to include the effects of 3D density structure as observed by CTD casts in May. The passive numerical drifters deployed in the vicinity of the front experienced a 5 m d^{-1} downwelling excursion to the lower half of the water column (Figure 6). Particles tended to converge from their original observation points to a narrow frontal region. Finally, the mooring records were assimilated into the model to provide a best estimate of the subtidal boundary elevations. This reduced the model versus observed velocity error from 0.128 to 0.084 m s^{-1} (Figure 7). The end result is shown in Figure 2(b) and (c). The distribution of numerical drifters (posted numbers) converged in the vicinity of the 60-m isobath, which roughly corresponds to the intersection of the front with the bottom. The fate of numerical particles is sensitive to the initial depths in the water column.

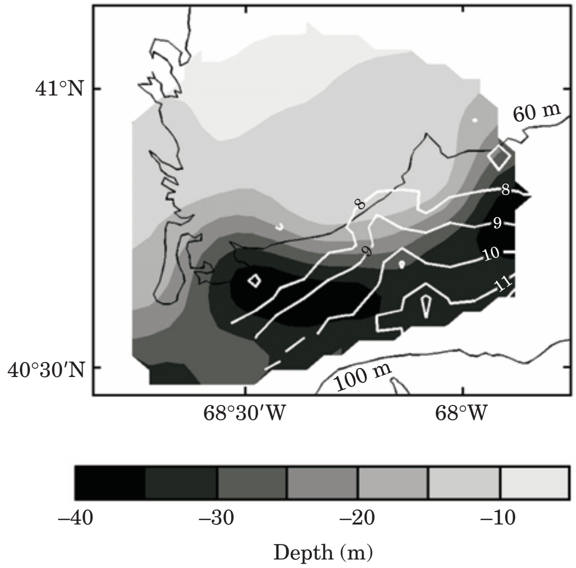

Figure 6. The depth of passive particles advected in the baroclinic flow field after 6 d (contoured). The bottom temperature front is overlaid as an indication of the frontal position and possible explanation of the downwelling that occurred. Note that some particles descended from 15 to >40 m.

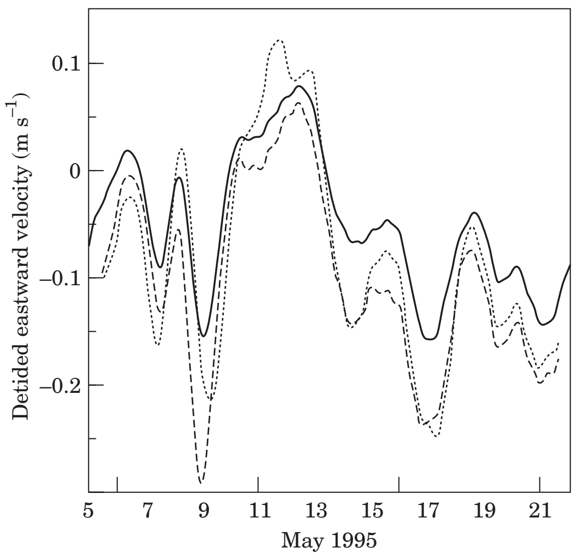

Figure 7. Observed (solid line) versus modeled subtidal flow at mooring site ST2 (broken line: best prior estimate from the QUODDY model runs; dotted line: final run after assimilation with subtidal boundary elevations included as forcing).

Discussion

Observations

The slope water intrusion of mid-May 1995 was possibly the most significant physical event of that spring on Georges Bank. An important question is how did the intrusion affect the population of young larval fish? More specifically, were the majority of larvae advected quickly towards the Mid-Atlantic Bight within the surface waters of the westward jet or were they simply "displaced" downward and shoalward toward the bank? The latter question cannot be answered directly because we cannot be sure that the concentrations observed in May represented the same individuals as those in April and March. Given an along-bank jet that is capable of transporting young larvae the entire length of Georges Bank in the space of a few weeks, it seems unlikely. Similar to the 1987 event, documented in Polacheck *et al*. (1992), an increase in geostrophic flow tends to transport particles along the shelf. However, given a mechanism for the animal to descend in the water column (Figure 6) either by physical downwelling (before getting trapped in the jet) or by the animal's own behavior, there are scenarios for retention.

The weighted-mean depth of the larvae differed significantly over each set of tows. The phase of the tide, the position of the haul relative to the front, time of day/night, and thermocline depth were all tested as possible forces that govern the animal's position in the water column, but no single variable provided a consistent explanation. Given the first drifter station alone, the variation of animal depth appeared consistent with tidal flow field, for example, but that relation failed to hold for subsequent stations.

Intensive sampling of Georges Bank physical and biological environment over the last few years has demonstrated a wider range of variability than previously recognized. Our efforts to quantify a seasonal process have been repeatedly thwarted by episodes of anomalous events. These results refer to one such event, a Gulf Stream ring causing a slope-water intrusion, which, in turn, evidently intensified the shelf-break jet. While the ring itself was centered a few hundred kilometers to the east, the leading edge apparently displaced slope water shoalward on to the bank as far as the 65 m isobath. The displacement of the shelf-slope front evidently caused a convergence and intensification of the normal along-bank flow in the form a 10 km wide shelf-break jet with residual velocities of 30 cm s^{-1} towards the west–southwest. Repeated cross-sections (CTD and ADCP) show this feature to be contained in the upper 30 m of the water column and located just shoalward of the front. A satellite track drifter that was apparently trapped in the jet logged 120 km in 5.5 d.

Modelling

Circulation models that can reproduce the complex flow along the southern edge of Georges Bank do not exist and may not exist for many years to come. However, models as implemented here can reproduce most of the variability given relatively simple input parameters and forcing. Given the additional baroclinic flow that was evident in mid-May 1995 (relative to climatology), numerical particles were advected both further to the west (Figure 8) and evidently downwelled deeper in the water column (Figure 6). The model results are improved further with the assimilation of moored velocity records (Figure 7). It is particularly important to simulate the effects of offshore eddy features on the southern flank of Georges Bank. Because synoptic observations of these processes are virtually impossible, they can only be inferred from the observed velocity within the interior of the grid.

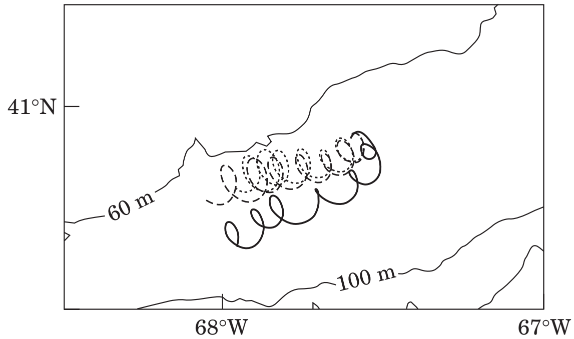

Figure 8. Particle tracks of observed (satellite tracked: solid line) and modeled (dashed: observed density; dotted: average climatological density) drifter centroids (mean position of four drifters for each time step) as a measure of the overall advection path (black dots: drifters start locations).

Results are presented here not as a realistic hindcast of the physical flow field but rather as an exercise in re-mapping biological distributions under particular scenarios. In the future, additional modeling exercises are needed to include the effects of processes not addressed so far. Surface heat flux, alternative parameterization of temperature and salinity at the boundary, feature models (such as an idealized Gulf Stream rings), are just a few examples of the sensitivity studies yet to be conducted.

In an attempt to demonstrate the biological consequences of the physical flow field, particles have been tracked through simulations. The direct comparison of a barotropic model run with moored current meter records just prior to the intrusion event shows the model accounting for most of the subtidal variability. After a set of preliminary tidal and barotropic runs, the Dartmouth Circulation Model is then initialized with the observed density field (which has been objectively fitted onto the model domain). A week-long baroclinic run is forced by multiple tides at the boundary and observed winds at the surface. The model then provides a more realistic simulation (relative to initialization with climatology). An additional improvement to the model results was obtained by assimilating moored velocity records within the model domain. These provide estimates of time-varying elevations around the boundary of the grid in an attempt to account for remote forcing. While still underestimating the intensity of the shelf-break jet, the model does provide a possible explanation for the observed concentrations of animals: convergence and downwelling of simulated particles near the frontal zone.

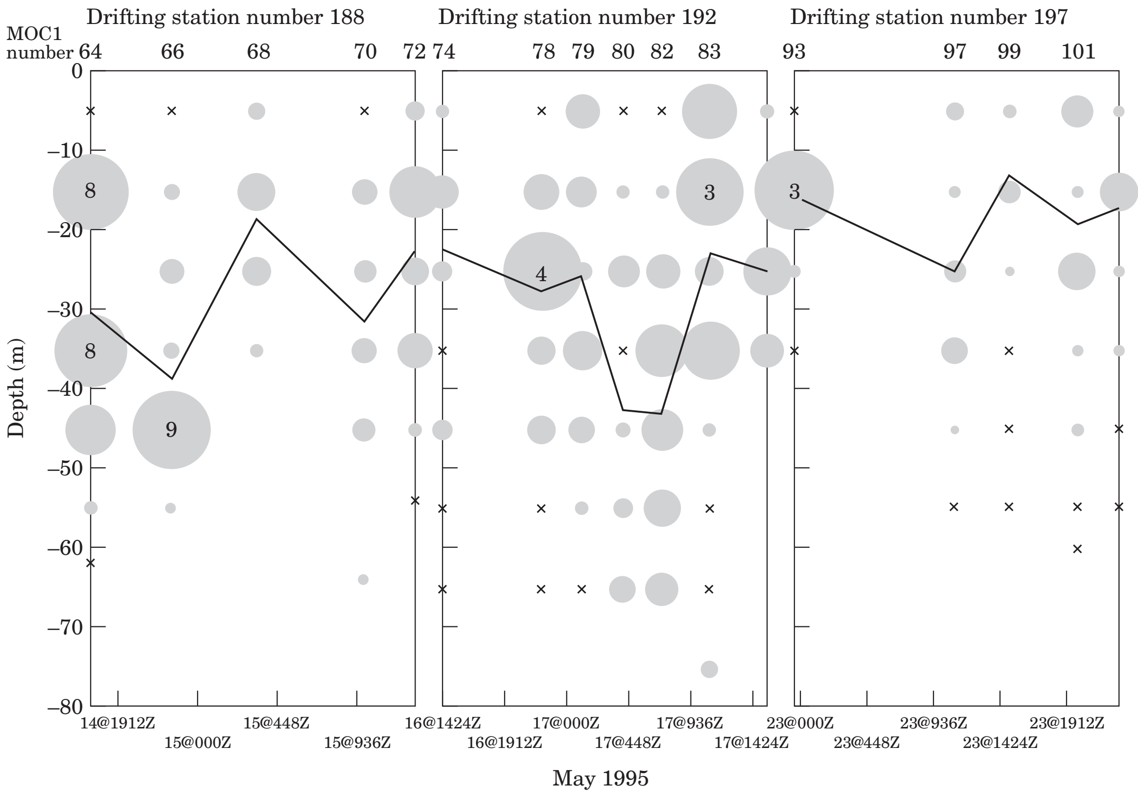

Figure 9. Vertical distribution and weighted-mean depth of larvae (cod+haddock) from 17 MOCNESS hauls conducted subsequent to the bongo grid on the on-bank side of the shelf-slope front at drifter stations 188, 192, and 197.

Acknowledgements

We thank all those aboard the RV "Seward Johnson" during the spring of 1995, in particular Betsy Broughton and Marie Kiladis for MOCNESS operations and Glenn Strout for drifter assistance. We also thank the entire crew (including the UMiami technicians) for providing a memorable experience on an ideal research platform. Jim Irish provided wind data from ST1. Charlie Flagg provided ADCP data from RV "Endeavor". Maureen Taylor and Bill Michaels provided additional CTD data from RV "Albatross IV" and RV "Katadin", respectively.

References

Bisagni, J. J., Beardsley, R. C., Rusham, C. M., Manning, J. P., and Williams, W. J. 1996. Historical and recent evidence of Scotian Shelf Water on Southern Georges Bank. Deep-Sea Research, 43: 1439–1471.

Blanton, B. 1993. User's Manual for 3-Dimensional Drogue Tracking on a Finite Element Grid with Linear Finite Elements. UNC Marine Science, Chapel Hill, North Carolina, USA.

Franks, P. J. S., and Chen, C. 1996. Plankton production in tidal fronts: a model of Georges Bank in summer. Journal of Marine Research, 54: 631–651.

Franks, P. J. S., and Walstad, L. J. 1997. Phytoplankton patches at fronts: a model of formation and response to wind events. Journal of Marine Research, 55: 1–29.

Garfield, N., and Evans, D. L. 1987. Shelf water entrainment of Gulf Stream warm-core rings. Journal of Geophysical Research, 92: 13993–14012.

Garvine, R. W., Wong, K.-C., Garwarkiewicz, G. G., and McCarthy, R. K. 1988. The morphology of shelf break eddies. Journal of Geophysical Research, 94: 14475–14483.

Griffin, D. A., and Thompson, K. R. 1996. The adjoint method of data assimilation used operationally for the shelf. Journal of Geophysical Research, 101: 3457–3477.

Greenberg, D. A., Loder, J. W., and Shen, Y. 1997. Spatial and temporal structure of the barotropic response of the Scotian Shelf and Gulf of Maine to surface wind stress: a model-based study. Journal of Geophysical Research, 102: 20897–20915.

Hannah, C. G., and Lynch, D. R. 1999. Casco3: User Guide. Numerical Methods Laboratory Document 99-6. Dartmouth College, Hanover, New Hampshire, USA.

Hannah, C. G., Loder, J. W., and Wright, D. G. 1996. Seasonal variation in the baroclinic circulation in the Scotia Maine Region. *In* Buoyancy Effects on Coastal and Estuarine Dynamics, 53, pp. 7–29. Ed. by D. Aubrey. American Geophysical Union Series.

Houghton, R. W., Schlitz, R., Beardsley, R. C., Butman, B., and Chamberlain, J. L. 1982. The Middle Atlantic Bight cold pool: evolution of the temperature structure during summer 1979. Journal of Physical Oceanography, 12: 1019–1029.

Houghton, R. W., Aikman III, F., and Ou, H. W. 1988. Shelf-slope frontal structure and cross-shelf exchange at the New England shelf-break. Continental Shelf Research, 8: 687–710.

Large, W. G., and Pond, S. 1981. Open ocean momentum flux measurements in moderate to strong winds. Journal of Physical Oceanography, 11: 324–336.

Linder, C. A. 1996. A climatology of the Middle Atlantic Bight shelfbreak front. MS thesis. Woods Hole Oceanographic Institute, Woods Hole, Massachusetts, USA.

Loder, J. W., and Wright, D. G. 1985. Tidal rectification and frontal circulation on the sides of Georges Bank. Journal of Marine Research, 43: 581–604.

Lough, R. G., and Trites, R. W. 1989. Chaetognaths and oceanography on Georges Bank. Journal of Marine Research, 47: 343–369.

Lynch, D. R., and Hannah, C. G. 2001. Inverse model for limited-area hindcasts on the continental shelf. Journal of Atmospheric and Oceanic Technology, 18: 962–981.

Lynch, D. R., Werner, F. E., Greenberg, D. A., and Loder, J. W. 1992. Diagnostic model for baroclinic, wind-driven, and tidal circulation in shallow seas. Continental Shelf Research, 12: 37–64.

Lynch, D. R., Ip, J. T. C., Naimie, C. E., and Werner, F. E. 1996. Comprehensive ocean circulation model with application to the Gulf of Maine. Continental Shelf Research, 16: 875–906.

Mountain, D. G., Strout, G. A., and Beardsley, R. C. 1996. Surface heat flux in the Gulf of Maine. Deep Sea Research, 43: 1533–1547.

Naimie, C. E., Loder, J. W., and Lynch, D. R. 1994. Seasonal variation of the three-dimensional residual circulation on Georges Bank. Journal of Geophysical Research, 99: 15967–15989.

Perry, R. I., Harding, G. C., Loder, J. W., Tremblay, M. J., Sinclair, M. M., and Drinkwater, K. F. 1993. Zooplankton distributions at the Georges Bank frontal system: retention or dispersion? Continental Shelf Research, 13: 357–382.

Petrie, B., Drinkwater, K., Gregory, D., Pettipas, R., and Sandstrom, A. 1996. Temperature and salinity atlas for the Scotian Shelf and Gulf of Maine. Canadian Technical Report of Hydrography and Ocean Sciences, 171: v+398 pp.

Pickart, R. S., Torres, D. J., McKee, T. K., Caruso, M. J., and Przystup, J. E. 1999. Diagnosing a meander of the shelfbreak current in the Mid-Atlantic Bight. Journal of Geophysical Research, 104: 3121–3132.

Polacheck, T., Mountain, D., Smith, W., and Berrien, P. 1992. Recruitment of the 1987 year class of Georges Bank haddock: influence of unusual larval transport. Canadian Journal of Fisheries and Aquatic Sciences, 49: 484–496.

Appendix

Assimilating moored velocity records to infer subtidal boundary elevations

As described in Hannah and Lynch (1999), a linearization of the Dartmouth QUODDY model (Lynch *et al.*, 1996) is inverted by means of steepest descent algorithms. The cost function is a weighted least squares blend of velocity mismatch plus the size (W0), slope (W1), and tendency (W2) of the elevations along the boundary (where the "tendency" refers to variability over time). The objective is to obtain the missing subtidal variance after having first simulated the effect of tides, local density structure, and wind. The output is intended to account for residual flow due to the far-field pressure forcing.

After an extensive model-tuning operation, inversion parameters 0, e^{12}, and e^{13} were selected for values of W0, W1, and W2, respectively. A temporal smoothing is dependent on a user selected time scale (in this case 6 h). To reduce the rms error of the model relative to the moored observations, we implemented a series of four QUODDY-CASCO runs to arrive at the minimized error. We noted the improved performance was limited to the region very near the mooring site and therefore the drogue paths were sensitive to the imposed velocity fields in other regions of the grid. Given the increased velocities near the adjusted boundary elements, the QUODDY model results become highly sensitive to the specification of temperature and salinity near the boundary. Allowing these state variables to change with the model values, rather than fixing them at initial conditions, modifies the density structure significantly. Obviously, more work is required on this aspect of the problem.